JOM, Vol. 72, No. 8, 2020
https://doi.org/10.1007/s11837-020-04179-4

Effect of Trace Silver on Precipitation Behavior of Strengthening Phases and Mechanical Properties of Aluminum-Copper Alloys

CONGCONG ZHU,[1] SHUAI WANG,[1] ZHIGANG WU,[2] and WENLI GAO[1,3]

1.—College of Materials Science and Engineering, Hunan University, Changsha 410082, China. 2.—Aerospace Research Institute of Special Material and Processing Technology, Beijing 100074, China. 3.—e-mail: wenligaohd@163.com

The effects of trace silver (Ag) on the precipitation behavior of strengthening phases and the mechanical properties of Al-Cu alloys have been investigated by performance testing, scanning electron microscopy, and transmission electron microscopy. Ag retarded the aging response of the Al-Cu alloys. The density of the θ'' and θ' phases decreased with increasing Ag content in under- and peak-aged alloys, and there was almost no θ' phase in the 0.12 wt.% Ag alloy in the under-aged state. The θ' phase morphology was narrower and longer after addition of Ag. Fatigue striations became more obvious and their spacing reduced at the fracture surface of experimental alloys with increasing Ag content, reflecting an improvement in the fatigue life of the alloys. On addition of 0.06 wt.% or 0.12 wt.% Ag, the fatigue life of the Al-Cu alloys was increased by 72.7% and 155.5%, respectively.

INTRODUCTION

Aluminum (Al)-copper (Cu) alloys are used extensively in aerospace and military industries as high-strength and high-toughness casting alloys, which can reduce the weight, improve the performance, and conserve raw materials and energy.[1] Al-Cu alloys are typical precipitation-strengthened materials whose properties can be improved by solid-solution and aging treatment. Most solute atoms dissolve in the alloy matrix during solid-solution treatment, forming a supersaturated solid solution after quenching. During aging, this supersaturated solid solution decomposes into fine and dispersed precipitated phases under a large driving force at a certain temperature.[2] Al-Cu alloys show excellent comprehensive performance after T6 peak-aging treatment, with the main strengthening phases being θ'' and θ'.[3] θ''-Al_3Cu has a distorted face-centered cubic structure consisting of two layers of Cu atoms separated by three layers of Al atoms; it precipitates coherently along the $\{001\}_{\alpha\text{-Al}}$ habit plane.[4] Meanwhile, θ'-Al_2Cu has a distorted CaF_2 structure that is coherent with $\{001\}_{\alpha\text{-Al}}$ and has the same orientation relationship with θ'' phase.[5]

With the development of materials science, researchers have found that the type, amount, size, and distribution of the strengthening phases directly affect the mechanical properties of alloys. Addition of trace amounts of alloying elements, i.e., microalloying elements such as scandium (Sc), silver (Ag), and cadmium (Cd), to Al-Cu alloys can change the morphology, distribution, and size of the precipitated phases.[6–8] Addition of elemental Ag has been found to enhance the mechanical properties by promoting Ω-phase precipitation in Al-Cu-magnesium (Mg) alloys and to decrease the width of the precipitate-free zones (PFZs) and increase the density of η' phase in Al-zinc (Zn)-Mg alloy, with no interaction between Ag and manganese.[9,10] Ag has a considerable influence on the aging response of Al-Cu-Mg alloys and enhances their strength.[11]

Ag addition promotes the formation of Ω phase on the α-Al matrix {111} surface, showing a thin hexagonal strip shape and being coherent with the matrix.[12] The Ω phase has an excellent aging strengthening effect and significantly enhances the high-temperature mechanical properties of Al-Cu-Mg alloys.[13] The mechanism underlying this effect of trace Ag on Al-Cu-Mg alloys is nanocluster-assisted promotion of precipitation. The nanoclusters that contain microalloying elements act as heterogeneous nucleation sites for subsequent precipitates. Ogura et al.[14] found that Ag atoms exhibit attractive interactions with solute (Zn and Mg) atoms and vacancies in Al-Zn-Mg alloys, which

(Published online May 1, 2020)

prevents vacancy diffusion to grain boundaries and enhances the nucleation rate. Therefore, the width of the PFZs was narrowed and the ductility of the aluminum alloy was improved. Lin et al.[15] found that trace Ag increased the density of η' precipitates and the Guinier–Preston (GP) zones in different aged conditions, which was responsible for the higher strength of Al-Zn-Mg alloys with Ag addition. γ'-$AlAg_2$ phase was present in Al-3.45 wt.% Ag-2.05 wt.% Cu alloy, but there was no γ' phase in Al-4.00 wt.% Cu-0.33 wt.% Ag alloy.[16] The effect of adding a small amount of Ag to Al-Cu alloys mainly results due to its significant segregation where θ' precipitates nucleate. This phenomenon whereby the precipitates are surrounded by Ag will affect the precipitation of the strengthening phase in Al-Cu alloys. Rosalie[17] found that Ag segregated to θ'-matrix interfaces in Al-Cu-Ag alloys. Elemental Ag segregated to coherent and semicoherent interfaces of θ' precipitates, forming an Ag-rich bilayer that impeded or prevented the growth of θ' precipitates.

Ag has been studied as a trace alloying element to enhance the mechanical properties of Al-Cu-Mg and Al-Zn-Mg alloys. However, ag exhibits different mechanisms of action on the precipitated phases of Al-Cu-Mg and Al-Zn-Mg alloys. The distribution of Ag in deformed Al-Cu alloys has been studied, but little attention has been paid to the effect of trace Ag on the mechanical properties and fatigue life of Al-Cu alloys. Therefore, the effect of trace Ag on the precipitation behavior of strengthening phases was investigated in this work, and the effect of trace Ag on the mechanical properties and fatigue properties of Al-Cu alloys is also discussed.

EXPERIMENTAL PROCEDURES

Experimental alloys were cast from high-purity raw material at 710°C utilizing a resin sand mold. Table I presents the chemical composition of each alloy. The concentrations of the component were detected by inductively coupled plasma-mass spectroscopy. The specimens were solid-solution treated at 538 ± 5°C for 17 h in a furnace, then quenched in normal ambient-temperature water. Artificial aging treatment was carried out in the furnace at 175 ± 5°C for different times (2 h to 35 h) to determine the peak aging time.

A Brinell hardness tester was used to measure the sample hardness, using a 10-mm-diameter indenter with a load of 1000 kgf for 30 s. The T6 heat-treated samples were subjected to tensile testing on a SANS-CMJ5105-type machine at loading speed of 2 mm/min and room temperature (~ 23°C). Fatigue testing was carried out using a QBG-100B high-cycle axial fatigue machine. Test samples were measured by high-frequency fatigue under axial loading at room temperature (~ 23°C) with loading stress of 100 MPa, $R = 0.1$, and $f = 120$ Hz. The average value of five effective experimental data points from the tensile and fatigue tests was used. The test samples are shown in Fig. 1. Scanning electron microscopy (SEM) images were obtained using a Philips FEGSEM at acceleration voltage of 30 kV and used to study the fracture morphology of the studied alloys. High-angle annular dark-field imaging in scanning transmission electron microscopy (HAADF–STEM) was applied to observe the precipitated phase along $<001>_{\alpha\text{-Al}}$ of the alloys with different Ag content. Specimens for STEM observation were prepared by ion-beam thinning. TEM and STEM observations were performed using a Tecnai G2 F20 S-TWIN microscope at acceleration voltage of 200 kV.

RESULTS

Hardness

The hardness curves of the investigated alloys with different Ag contents during artificial aging at 175 ± 5°C are presented in Fig. 2. The three as-quenched alloys showed almost the same hardness values, indicating that addition of small amounts of Ag did not affect the solid-solution strengthening of the studied alloys. The three alloys showed similar changes during the subsequent artificial aging process. The alloy hardness increased with time until a peak value was reached, then the values decreased and tended to stability. The Ag-free alloy peaked at 148 HBW after 6 h of aging treatment, whereas the 0.06 wt.% Ag alloy showed a peak of 145 HBW after aging for 8 h and the 0.12 wt.% Ag alloy reached a maximum hardness of 139 HBW after aging for 12 h. This difference reveals that addition of Ag decreased the peak hardness value and suppressed the age-hardening response.

Mechanical Properties

Figure 3 shows that addition of trace Ag had an important effect on the mechanical properties of the studied alloys; For instance, the tensile strength decreased from 461.6 MPa to 452 MPa after added 0.06 wt.% Ag, then to 401 MPa with 0.12 wt.% Ag addition. The yield strength also decreased with Ag addition. However, there was an opposite trend in

Table I. Chemical composition (in wt.%) of each experimental alloy

	Cu	Mn	Ti	Zr	V	B	Cd	Ag	Al
Alloy 1	5.00	0.42	0.20	0.11	0.2	0.01	0.19	0	Bal.
Alloy 2	4.98	0.42	0.19	0.12	0.22	0.009	0.20	0.06	Bal.
Alloy 3	4.99	0.41	0.18	0.12	0.22	0.009	0.19	0.12	Bal.

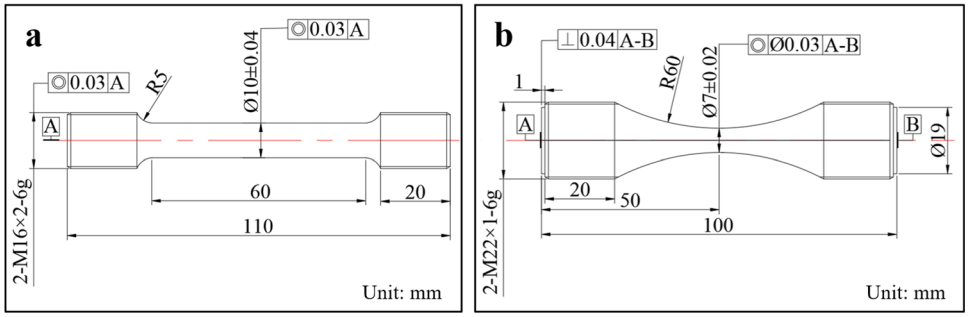

Fig. 1. Schematic of specimens: (a) tensile test specimen at room temperature; and (b) high-cycle axial fatigue test specimen at room temperature.

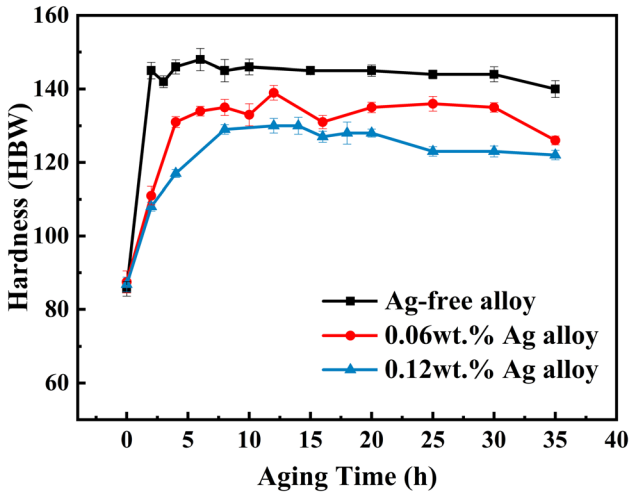

Fig. 2. Brinell hardness values of studied alloys as function of aging time at 175°C.

the ductility. The elongation of the Al-Cu alloys increased significantly with increasing Ag content, from 1.38% to 1.9% with 0.06 wt.% Ag addition, reaching 3.5% with 0.12 wt.% Ag addition. These results suggest that addition of trace Ag could improve the plasticity and toughness but decrease the strength of Al-Cu alloys.

Fatigue Life

Figure 4 indicates that the fatigue life of the studied alloys increased with Ag addition. Under the same test condition, the fatigue life of the Ag-free alloy was 1.1×10^6 cycles, while that of the 0.06 wt.% Ag alloy reached 1.9×10^6 cycles, and the 0.12 wt.% Ag alloy showed a fatigue life of 2.8×10^6 cycles. The fatigue life of the Al-Cu alloys was increased by 72.7% on 0.06 wt.% Ag addition and by 155.5% when the Ag content reached 0.12 wt.%. These experimental data show that trace Ag addition could ameliorate the fatigue life of Al-Cu alloys.

Figure 5 shows the fatigue fracture morphology of the experimental alloys after the high-cycle axial fatigue test. The alloys with different Ag contents showed different features of cleavage steps and fatigue striations. The fatigue fringes on the fatigue fracture surfaces of the alloys with different Ag contents were analyzed to understand the effect of Ag addition clearly. The number of fatigue fringes within the same distance was counted to calculate the average distance between adjacent fatigue fringes. Many cleavage steps and some fatigue striation characteristics in the Ag-free alloy are shown in Fig. 5a. According to the statistical results, the distance between adjacent fatigue fringes was 5.56 μm in the Ag-free alloy. Figure 5b shows that the cleavage steps decreased while fatigue striations were obvious and the distance between adjacent fatigue fringes reduced to 3.13 μm, indicating that the alloy with 0.06 wt.% Ag had better toughness. In Fig. 5c, the cleavage-step characteristics are weak while the ridges of the fatigue striations are obvious. The number of fatigue striations continued to increase while their distance decreased. In the 0.12 wt.% Ag alloy, the distance between adjacent fatigue fringes was only 2.38 μm, indicating that addition of 0.12 wt.% Ag improved the alloy toughness. These changes in the fatigue fracture morphology indicate that trace Ag had a significant effect on the fatigue properties of the studied alloys.

Precipitation-Strengthening Phases

Figure 6 shows typical STEM micrographs and corresponding selected-area electron diffraction (SAED) patterns of precipitates in the studied alloys after 2 h of artificial aging. The appearance of the diffraction patterns in Fig. 6a, b, and c remained unchanged, confirming that Ag addition did not affect the habit plane of the precipitated phase. The SAED patterns in Fig. 6a, b, and c taken from smaller precipitates embedded in the α-Al matrix show discontinuous streaks through the $\{020\}_{\alpha\text{-Al}}$ SAED pattern with the maximum intensities of the streak located at $\{010\}_{\alpha\text{-Al}}$ (marked by yellow arrow).

The characteristics of the diffraction pattern and the phase structure confirm that the small precipitates were θ'' phases. The θ' feature in the SAED pattern in Fig. 6a is indicated by the red arrow. The microstructure of the different investigated alloys near the $[001]_{\alpha\text{-Al}}$ zone axis was characterized by plate-like precipitates. Two type of structures of θ'

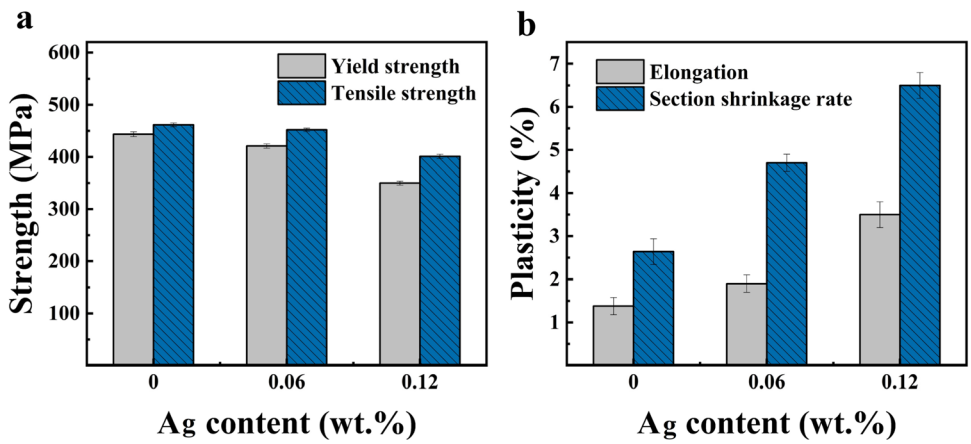

Fig. 3. Mechanical properties of studied alloys after peak aging treatment: (a) strength and (b) plasticity.

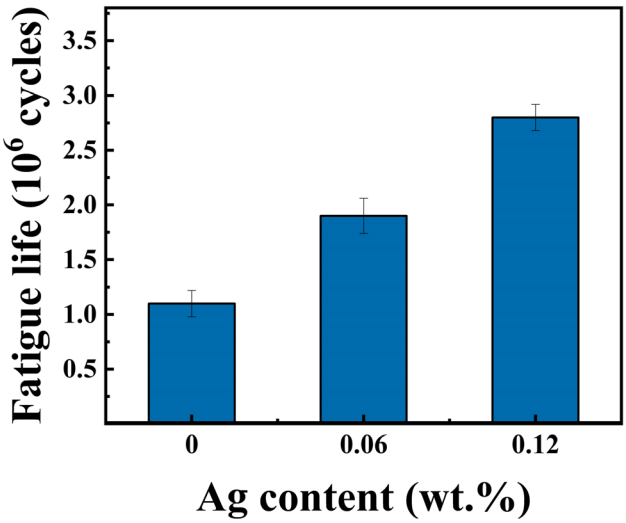

Fig. 4. Fatigue life of experimental alloys in peak-aged state under axial high-cycle fatigue.

observed in the studied alloys are shown in Fig. 6d and e. Figure 6a shows a STEM image of the Ag-free alloy. The main precipitation phase was θ'', while a small amount of θ' phase was present. The content of both θ'' and θ' decreased when 0.06 wt.% Ag was added, as shown in Fig. 6b. In the 0.12 wt.% Ag alloy in Fig. 6c, the number of θ'' phases continued to decrease and there was almost no θ' phase.

Figure 7 shows STEM micrographs of the alloys with different Ag content after peak aging. It is seen that the long strip-like precipitated phase correspond to θ' precipitates (marked by red arrow) while the short phase corresponded to the θ'' precipitates (marked by yellow arrow) seen in Fig. 6d, e, and f. The number density of θ'' and θ' phases decreased with Ag addition. The θ' phase narrowed and lengthened, as shown in Fig. 7a, b, and c. Therefore, the inhibition effect of Ag on the aging of the Al-Cu alloys was long acting. Figure 7g, h, and i show that the PFZ width was 96.2 nm, 90.51 nm, and 92.65 nm for the Ag-free, 0.06 wt.% Ag, and 0.12 wt.% Ag alloy, respectively. This illustrates that Ag did not affect the PFZs of the experimental alloys.

DISCUSSION

Influence of Ag Addition on Precipitation

Supersaturated solid solution (SSS) → Guinier–Preston (GP) zones → GP II zones (θ'') → metastable phase (θ') → equilibrium phase (θ) is acknowledged to be the evolutionary process for describing the fundamental theory of precipitation hardening in Al-Cu alloys.[18] HAADF images along $<100>_{\alpha\text{-Al}}$ were captured to observe the plate-like θ'' and θ' precipitates. A small amount of Ag addition decreased the density of θ'' and θ' precipitates in the under-aged condition, suggesting that trace Ag in the Al-Cu alloy influenced its age-hardening performance. In Fig. 7a, b, and c, both θ'' and θ' precipitates were observed among the studied alloys after peak-aging treatment. This observation indicates that the precipitates are the main strengthening phases in the peak-aged condition, similar to the results of Bourgeois.[19] The STEM and SAED results showed that addition of Ag did not change the type of precipitated phase or the habit plane of the precipitates, as shown in Fig. 6. However, the density of θ'' and θ' precipitates decreased after peak-aging treatment, and the θ' phase was narrower and longer, as shown in Fig. 7b. Figure 7g, h, and i show that the width of the PFZ zones of the alloys did not change after addition of elemental Ag. The grain boundary is a highly disordered region composed of many dislocations, and nearby Cu atoms diffuse mainly into the grain boundary along dislocation lines.[20] Elemental Ag has little effect on such diffusion of Cu atoms near the grain boundary. Therefore, the effect of elemental Ag on the precipitation of the strengthening phase at the grain boundary is not obvious. In summary, the

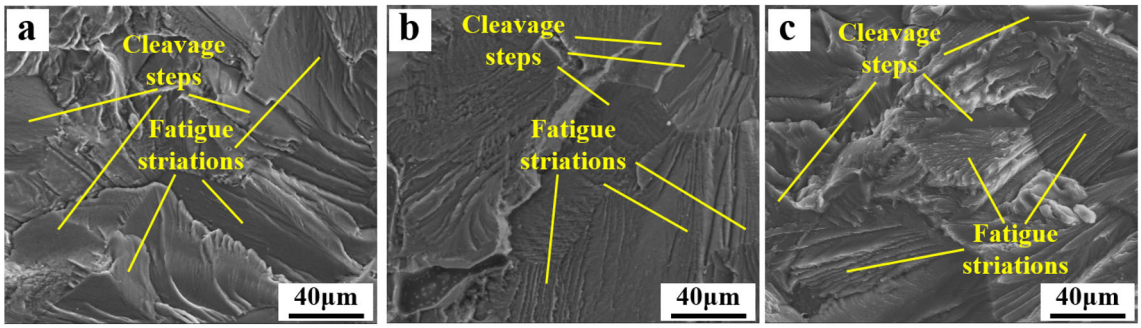

Fig. 5. Fatigue fracture morphology of high-cycle axial fatigue test samples of (a) Ag-free, (b) 0.06Ag, and (c) 0.12Ag alloys after peak aging.

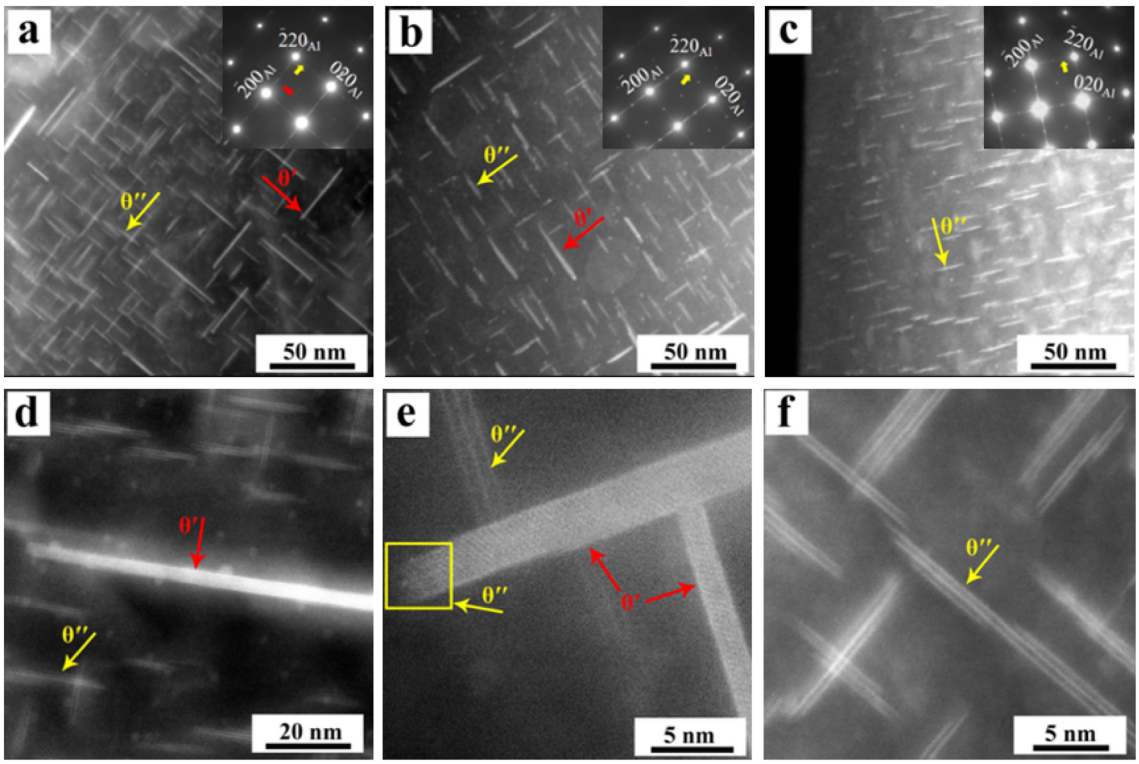

Fig. 6. Representative STEM micrographs after 2 h of artificial aging treatment showing the microstructure in (a) Ag-free, (b) 0.06Ag, and (c) 0.12Ag alloys; (d)–(f) Morphology of θ'' and θ' phases of experimental alloys.

change in the strengthening phases was responsible for the change in the mechanical properties of the Ag-containing alloys.

The age-hardening curves in Fig. 2 show that addition of 0.06 wt.% or 0.12 wt.% Ag to the Al-Cu alloy retarded its aging response. One reasonable interpretation for the precipitation is associated with the presence of vacancies, which have an important effect on precipitation processes in age-strengthened aluminum alloys[21,22] Cu atom migration during aging occurs mainly via vacancies. In the vacancy cluster mechanism developed by Ozawa,[23] vacancy clusters are considered to form first and then act as locations for favored nucleation of precipitates. Solute atoms that combine with vacancies have an obvious impact on the aging process and precipitate nucleation. Figure 6 shows that the θ'' phase precipitation gradually reduced with Ag addition after the same aging time of 2 h (under-aging). It is considered that Ag inhibited the aging response of the Al-Cu alloys. Ag atoms affected the diffusion of Cu atoms in the alloy. On the one hand, the energy of vacancy generation will increase after Ag element addition, leading to a decrease in the number of vacancies in the alloy and thereby inhibiting the diffusion and migration of Cu atoms.[24] On the other hand, the obvious change observed in the aging behavior after addition of Ag can be interpreted by considering solute–vacancy interactions. The interaction energy between Cu

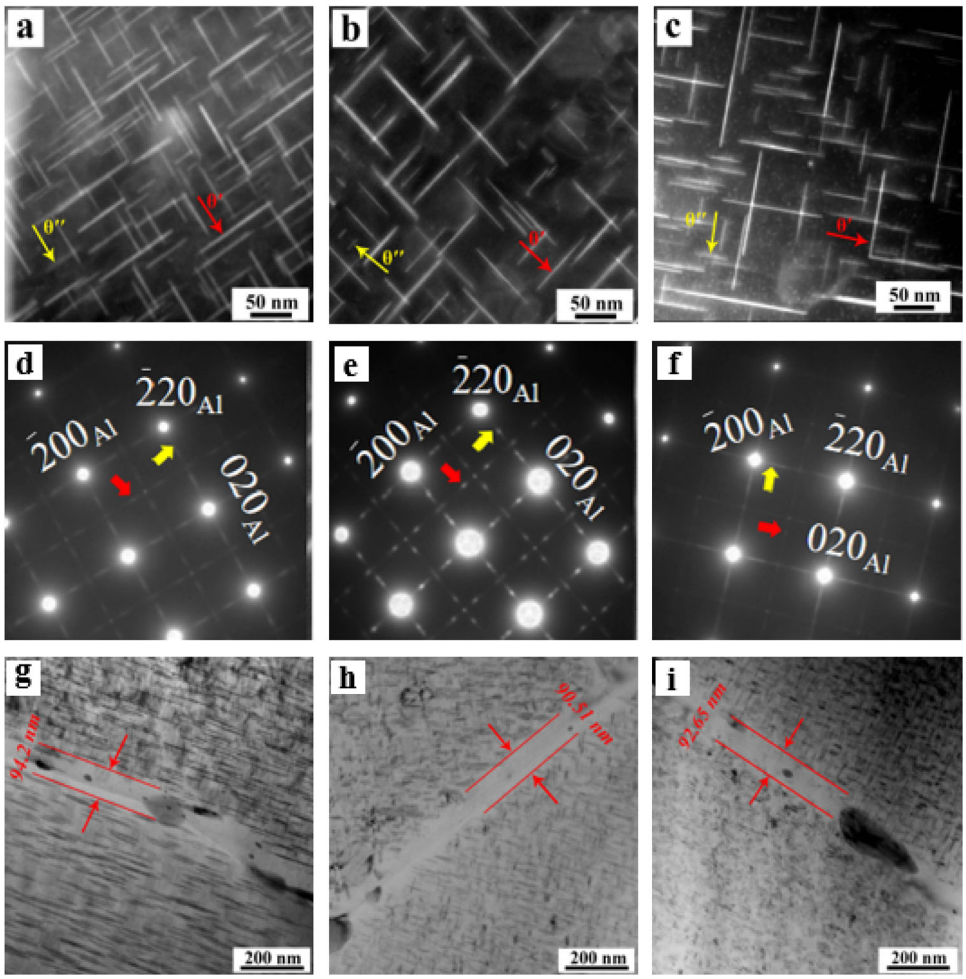

Fig. 7. Representative STEM micrographs under peak aging showing the precipitation in (a) Ag-free, (b) 0.06Ag, and (c) 0.12Ag alloys; (d)–(f) corresponding SAED patterns and (g)–(i) TEM images showing the PFZ width.

atoms and vacancies is 0.5 eV, while the energy between Ag atoms and vacancies is − 0.8 eV.[25] These positive and negative signs indicate repulsive and attractive interactions, respectively. Therefore, Ag atoms will preferentially combine with vacancies during the aging process. The radius of the Ag atom is greater than that of the Cu atom, so Ag atoms occupy more space, further reducing the concentration of vacancies in the matrix. Both of these factors hinder migration of Cu atoms. Huang[20] and Ringer[26] proved that there was almost no interaction between Ag and Cu, so there are no Cu-Ag-vacant clusters. Ag failed to promote the migration of Cu atom by capturing Cu atoms to form GP zones and precipitates. The θ'' phase is an intermediate transition phase formed during atom ordering in the GP zones and remains coherent with the aluminum matrix. The occupation of vacancies by Ag atoms and the inhibition of Cu atom migration will lead to a reduction of the θ'' phase, as shown in Fig. 6. Some θ' phases were observed in the Ag-free alloy after aging for 2 h, as shown in Fig. 6a. The θ' phase decreased with addition of 0.06 wt.% Ag as seen in Fig. 6b, and there was almost no θ' phase when the Ag content reached 0.12 wt.%, as seen in Fig. 6c. This reflects the fact that Ag suppressed the precipitation of θ' phase and that this inhibitory effect increased with increasing Ag content.

Figure 7a, b, and c show the morphology and distribution of the precipitated phases of the Ag-free, 0.06 wt.% Ag, and 0.12 wt.% Ag alloys after peak aging. The number of θ'' and θ' phases decreased with increasing Ag content. This result further confirms the long-term effect of Ag in inhibiting the precipitates in the Al-Cu alloy, corresponding to the variation in the age-hardening curves seen in Fig. 2. Addition of Ag inhibited formation of GP zones in the Al-Cu alloys, resulting in the decrease in the number of θ' phases. There are two modes of nucleation and growth for θ' phase.[27] One is formation of heterogeneous nucleation at high-energy locations such as defects or dislocations. The other is due to continuous enrichment and rearrangement of Cu atoms in θ'' phase. It is difficult for θ' phase to nucleate heterogeneously on dislocations or vacant clusters with Ag addition, because it has a large misfit energy at semicoherent interfaces with the matrix.[28] Thus, θ' phases

precipitated heterogeneously in the alloys with added Ag after peak-aging treatment. The morphology of θ' generated by this mechanism was more susceptible to the influence of elemental Ag. Moreover, more vacancies would be occupied and the inhibitive effect on GP formation would be stronger with increasing Ag content. As a result, less precipitation of θ' phase will occur in the alloy, as seen in Fig. 7. Silcock et al.[29] proved that θ' cannot transform into θ at an aging temperature of 175°C. Therefore, these results confirm that Ag inhibited the entire aging process of the Al-Cu alloys. Figure 7a, b, and c show the change in the θ' morphology with Ag addition. According to the results of Rosalie,[17] Ag segregated on θ' phase coherent and semicoherent surfaces and formed a two-atom-wide layer, which will affect the growth of θ' phase. The segregation energy of an Ag atom at the θ' phase coherent interface with Al_i is − 0.01 eV and with Al_{i-1} is − 0.04 eV, while the value for Cu at the θ' phase coherent interface with Al_i is 0.04 eV and with Al_{i-1} is 0.01 eV.[30] Meanwhile, Ag shows high solid solubility in the aluminum matrix and is therefore more likely to segregate on the θ' phase coherent surface and form a layer two atoms thick.[16] However, Cu atoms have a more negative value at the θ' phase semicoherent interface with Al_i and Al_{i-1} compared with Ag atoms. It was not easy for Ag atoms to segregate at the semicoherent interface of the θ' phase. The partial convergence of Ag atoms reduces the interfacial energy between the coherent interface of θ' phase and the matrix. The segregation of Ag atoms at the θ'-matrix coherent interface hinders the segregation of Cu atoms, thus affecting the transverse growth of the θ' phase. This explains why the θ' phase precipitated in the Al-Cu alloys became finer and longer after Ag addition. The density of θ' and θ'' decreased and the morphology of the θ' phase changed after Ag addition.

Effect of Ag Addition on Mechanical Properties and Fatigue Life of Alloys

Figure 7 shows that the density of the θ'' and θ' precipitates decreased, while the θ' phase became narrower and longer, with increasing Ag content. This decrease of the precipitated phases will reduce the accumulation of dislocations during the deformation process, thereby decreasing the stress concentration and resulting in stress relaxation, which will facilitate dislocation slip, while the narrower θ' phase could also reduce the stress concentration during deformation. Therefore, the alloy will be more evenly stressed during deformation. More deformation will therefore occur for a given force, indicating an improvement in the ductility. The weakening of the dislocation pinning would reduce the strength of the experimental alloys. The increase in the strength of precipitation-strengthened alloys containing <100> plate-like phases can be expressed using the Orowan formula:[31]

$$\sigma = \frac{2Gb}{2\pi(1-\upsilon)^2}\frac{1}{\lambda}\ln\frac{D}{d}$$

where b is the Burgers vector, G is the matrix shear modulus, υ is the Poisson ratio, λ is the precipitated phase spacing, D is the initial particle radius, and d is the average size of the precipitated phase. For the studied alloys, G, b, υ, and D are fixed. The lengthening of θ' will increase d, while the decrease in the θ'' and θ' precipitates will cause an increase in λ, resulting in a decrease in the strength σ of the Ag-containing alloys. Ag addition inhibited the precipitation of the strengthening phase in the studied alloys, resulting in greater Cu atom retention in the alloy matrix. This will enhance the solid-solution strengthening and contribute to the improvement of the strength and toughness in the Al-Cu alloys. However, the experimental alloys exhibited a more significant improvement in strength from the precipitated θ'' and θ' phases, so the ductility of the Ag-containing alloy was improved but with a slight decrease in strength resulting from the residual Cu in the Al matrix. Figure 7g, h, and i confirm that the PFZ width of the studied alloys remained unchanged, indicating that addition of trace Ag will not affect the precipitation of the strengthening phases at grain boundaries. Therefore, the change of the ductility is independent of the PFZs in the investigated alloys.

A strengthening phase can hinder dislocation slip in Al-Cu alloys. Dislocation stacks on the θ'' and θ' phase result in stress concentrations under cyclic loading. When the stress concentration exceeds the barrier fracture strength or the bond strength with the matrix, the barriers will break or separate from the matrix along the θ''/θ'-matrix interface.[32] This mechanism provides a preferential path for fatigue crack growth, reducing the energy required for fatigue crack growth and facilitating crack expansion.[33] The density of θ'' and θ' phases decreased, so that the stress concentration was weakened and the stress distribution became more uniform during deformation. As a result, the growth rate of the fatigue crack will be retarded. Ag segregation at the coherent surface of θ' phase was not conducive to dislocation pinning during deformation, hindering fatigue-crack initiation and improving the fatigue properties of the 0.06 wt.% and 0.12 wt.% Ag alloys. The ductility of the alloys increased with Ag addition, so the crack tip was passivated easily under cyclic loading. The crack propagation distance decreased during each cyclic period, as manifested by the decrease in the spacing of the fatigue striation seen in Fig. 5, thus the crack growth rate decreased.

A change in the shape of the strengthening phase in the experimental alloys was mainly seen for the θ' phase after peak aging. The θ' phases have a short and rough appearance in Fig. 7a. This shape is not easily sheared by dislocations during deformation,

so dislocations will bypass the θ' phase and form an Orowan ring around it.[34] In this situation, deformation proceeds in a double-slip mode, which straightens the expansion path, thus facilitating crack expansion. The narrower θ' precipitates were easily sheared by the slip zone of the fatigue-crack front in Fig. 7b and c. In this situation, dislocations slide mainly along the sliding system in the grain during deformation, making the crack path in the alloys serrated and tortuous in this single shear-failure mode. Therefore, the fatigue-crack growth rate of the alloy decreased while the fatigue life increased. Suresh et al.[35] proposed a bridging effect in which the long second phase contacts the crack surface, resulting in crack closure during unloading. Thus, the increase of θ' phase in the Al-Cu alloys with Ag addition could improve the fatigue crack closure and reduce the effective driving force for crack growth, as manifested by the increase of the fatigue life of the Ag-containing alloys seen in Fig. 4.

CONCLUSION

The effects of adding trace amounts (0.06 wt.% or 0.12 wt.%) of Ag on the microstructure and mechanical properties of Al-Cu alloys were investigated, revealing an obvious influence on the precipitated phases and mechanical properties after peak-aging treatment. The following conclusions can be drawn from this work:

1. Addition of small amounts of Ag to Al-Cu alloy suppressed the age-hardening effect and prolonged the time to peak aging. However, increasing Ag content had no effect on the PFZ width.
2. Addition of Ag inhibited formation of θ'' and θ'. The density of θ'' and θ' phases decreased with Ag addition in both the under- and peak-aged Al-Cu alloys. There was almost no θ' phase in the under-aged Al-Cu alloy with 0.12 wt.% Ag addition.
3. The plasticity of the Al-Cu alloys was enhanced while their strength was weakened after addition of trace amounts of Ag. The cleavage step features became less visible, the ridges of the fatigue striations became more obvious, and the striation spacing was reduced at the fracture surface of the studied alloys with increasing Ag content. The fatigue life of the investigated alloys was increased by 72.7% after addition of 0.06 wt.% Ag and by 155.5% after addition of 0.12 wt.% Ag.

ACKNOWLEDGEMENTS

The authors acknowledge financial support of the National Natural Science Foundation of China (Nos. 51474101, 51271076 and 51474195) and the Aluminum Alloy Laboratory of Beijing Institute of Aeronautical Materials.

CONFLICT OF INTEREST

The authors declare that they have no conflict of interest.

REFERENCES

1. Z. Chen, Q. Shu, and Y. Chen, *Mater. Sci. Technol.* 15, 718 (2007).
2. Y. Chen, W. Liu, and S. Yuan, *JOM* 67, 938 (2015).
3. Y. Ando, K. Mihama, T. Takahashi, and Y. Kojima, *J. Cryst. Growth* 24–25, 581 (1974).
4. Z. Shen, Q. Ding, C. Liu, J. Wang, H. Tian, J. Li, and Z. Zhang, *J. Mater. Sci. Technol.* 33, 1159 (2017).
5. D. Porter, E. Kenneth, and M. Sherif, *Transformations in Metals and Alloys*, 3rd ed. (London: Taylor & Francis, 1992).
6. R. Lumley and I. Polmear, *Scr. Mater.* 50, 1227 (2004).
7. T. Sato, S. Hirosawa, K. Hirose, and T. Maeguchi, *Metall. Mater. Trans. A* 34, 2745 (2003).
8. B. Sofyan, I. Polmear, and S. Ringer, *Mater. Sci. Forum* 396–402, 613 (2002).
9. D. Xiao, J. Wang, D. Ding, and S. Chen, *J. Alloys Compd.* 343, 77 (2002).
10. S. Maloney, I. Polmear, and S. Ringer, *Mater. Sci. Forum* 396–402, 631 (2002).
11. K. Hono, N. Sano, S. Babu, R. Okano, and T. Sakurai, *Acta Mater.* 41, 82 (1993).
12. A. Mukhopadhyay, G. Eggeler, and B. Skrotzki, *Scr. Mater.* 44, 545 (2001).
13. W. Rainforth, L. Rylands, and H. Jones, *Scr. Mater.* 35(2), 261 (1996).
14. T. Ogura, A. Hirose, and T. Sato, *Mater. Sci. Forum* 638, 297 (2010).
15. L. Lin, Z. Liu, W. Liu, Y. Zhou, and T. Huang, *J. Mater. Sci. Technol.* 34, 534 (2018).
16. J. Rosalie, L. Bourgeois, and C. Muddle, *Light Metals* (Springer, 2012), pp. 307–312.
17. J. Rosalie and L. Bourgeois, *Acta Mater.* 60, 6033 (2012).
18. W. Gayle and M. Goodway, *Science* 266, 1015 (1994).
19. L. Bourgeois, C. Dwyer, M. Weyland, J. Nie, and B. Muddle, *Acta Mater.* 60, 633 (2012).
20. B. Huang and Z. Zheng, *Acta Mater.* 46, 4381 (1998).
21. S. Bai, X. Zhou, Z. Liu, P. Ying, M. Liu, and S. Zeng, *Mater. Sci. Eng. A* 637, 183 (2015).
22. S. Pogatscher, E. Kozeschnik, H. Antrekowitsch, M. Werinos, S. Gerstl, J. Löffler, and P. Uggowitzer, *Scr. Mater.* 89, 53 (2014).
23. E. Ozawa and H. Kimura, *Acta Mater.* 18, 995 (1970).
24. S. Zufiqar, H. Sardar, Z. Rehman, R. Sardar, and B. Farida, *Surf. Rev. Lett.* 21, 1450072 (2014).
25. S. Hirosawa, F. Nakamura, and T. Sato, *Mater. Sci. Forum* 561–565, 283 (2007).
26. S. Ringer, K. Hono, I. Polmear, and T. Sakurai, *Acta Mater.* 44, 1883 (1996).
27. D. Vaughan, *Acta Mater.* 16, 563 (1968).
28. A. Suzuki and H. Kimura, *Mater. Sci. Eng.* 6, 384 (1970).
29. M. Silcock, J. Heal, and K. Hardy, *J. Inst. Met.* 82, 239 (1954).
30. D. Shin, A. Shyam, S. Lee, Y. Yamamoto, and J. Haynes, *Acta Mater.* 327–340, 141 (2017).
31. H. Liu, Y. Gao, L. Qi, Y. Wang, and J. Nie, *Metall. Mater. Trans. A* 46, 3287 (2015).
32. D. Broek, *Eng. Fract. Mech.* 5, 55 (1973).
33. G. Zhang, G. Liu, X. Ding, J. Sun, Z. Tong, Y. Shao, and K. Chen, *Rare. Met. Mater. Eng.* 33, 35 (2004).
34. Y. Liu, Z. Liu, Y. Li, Q. Xia, and J. Zhou, *Mater. Sci. Eng. A* 492, 333 (2008).
35. S. Suresh and R. Ritchie, *Int. Mater. Rev.* 29, 445 (2013).